A R C H I V E S O F M E T A L L U R G Y A N D M A T E R I A L S
Volume 57 2012 Issue 3
DOI: 10.2478/v10172-012-0069-5

K. STAN*, L. LITYŃSKA-DOBRZYŃSKA*, A. GÓRAL*, A. WIERZBICKA-MIERNIK*

CHARACTERIZATION OF AS-SPUN AND ANNEALED Al-Mn-Fe RIBBONS

CHARAKTERYSTYKA SZYBKO CHŁODZONYCH TAŚM STOPU Al-Mn-Fe W STANIE WYJŚCIOWYM ORAZ PO WYGRZEWANIU

Microstructure of conventionally cast and melt spun $Al_{91}Mn_7Fe_2$ alloy was examined by X-ray diffraction, SEM and TEM techniques. Three different phases were found in a mould cast ingot: Al_6(Mn, Fe), Al_4(Mn, Fe) and aluminium solid solution. Rapidly quenched ribbons cast using melt spinning technique with different speed values of rotating wheel: 25, 30 and 36 m/s had average width in a range of 30-50 μm. It was found that ribbons contain quasicrystalline particles with different sizes and shapes including large dendrites in a range of micrometers and smaller spherical particles below 1 μm embedded in an aluminium matrix. Composition of these particles was similar to the Al_4(Mn, Fe) phase. Also quasicrystals in the form of eutectic were observed with slightly different composition close to the Al_6(Mn, Fe) phase. All observed particles revealed 2, 3 and 5- fold symmetry, typical for icosahedral quasicrystals. Increase in microhardness up to 274 HV for melt spun ribbon comparing to 141 HV for the as-cast ingot was observed due to a change in phase composition and refinement of the phases. Thermal stability of quasicrystalline phase in the ribbon was examined by annealing in different temperatures. Temperatures for thermal treatment were chosen based on DSC curve which contains the exothermic peak in the temperature range 300-500°C. Analysis of ribbons annealed for 30 minutes at 400°C showed that transformation of quasicrystals to stable crystalline phase starts at quasicrystal/Al-matrix interfaces. After annealing for 4 hours at 500°C only the Al_6(Mn, Fe) phase and aluminium solid solution were observed in the ribbon microstructure.

Keywords: Al-Mn-Fe, quasicrystals, melt-spinning, DSC, TEM

Mikrostrukturę stopu $Al_{91}Mn_7Fe_2$ odlanego do kokili oraz przygotowanego metodą odlewania na wirujący walec (melt spinning) scharakteryzowano za pomocą dyfrakcji rentgenowskiej oraz transmisyjnej i skaningowej mikroskopii elektronowej. W strukturze wlewka zaobserwowano trzy fazy: Al_6(Mn, Fe), Al_4 (Mn, Fe) oraz roztwór stały aluminium. Szybko chłodzone taśmy odlano przy trzech różnych prędkościach obracającego się walca: 25, 30 i 36 m/s. Grubość wszystkich otrzymanych taśm wynosiła około 30-50 μm. Mikrostruktura taśm składała się z cząstek kwazikrystalicznych o zróżnicowanych kształtach i rozmiarach (w tym dużych dendrytów rzędu kilku mikrometrów, oraz mniejszych kulistych cząstek poniżej 1μm). Skład chemiczny tych cząstek był zbliżony do składu fazy Al_4(Mn, Fe). Zaobserwowano również kwazikryształy w postaci eutektyki o składzie zbliżonym do składu fazy Al_6(Mn, Fe). Uzyskane dyfrakcje elektronowe z obserwowanych cząstek wykazywały symetrię 2, 3 i 5-krotną, typową dla kwazikryształów ikozaedrycznych. Zmiany składu fazowego oraz rozdrobnienia faz spowodowały wzrost mikrotwardości z 140 HV dla stopu wyjściowego do wartości 270 HV dla taśm. Stabilność termiczną fazy kwazikrystalicznej badano poprzez wygrzewanie taśm w różnych temperaturach, które wybrano w oparciu o krzywą DSC zawierającą pik egzotermiczny w przedziale temperatur 300-500°C. Analiza mikrostruktury taśmy wygrzewanej przez 30 min w 400°C wykazała, że przemiana fazy kwazikrystalicznej w stabilną fazę krystaliczną rozpoczyna się na granicy kwazikryształ/osnowa. Po wygrzewaniu przez 4 godz. w 500°C w strukturze taśmy występowała jedynie faza Al_6(Mn, Fe) oraz roztwór stały aluminium.

1. Introduction

High strength aluminium-based alloys achieved great importance for advanced structural applications in aerospace and transportation industries because of their low density and high corrosion resistance. During the last decade a considerable effort has been devoted to the development of a new group of materials consisting of quasicrystalline particles embedded in an aluminium matrix because of their promising properties [1-9]. Quasicrystals exhibit a unique combination of physical properties: low thermal and electrical conductivity, unusual optical and magnetic properties, low surface energy and friction coefficient, high strength and hardness, high

* INSTITUTE OF METALLURGY AND MATERIALS SCIENCE POLISH ACADEMY OF SCIENCES, 30-059 KRAKÓW, 25 REYMONTA STR., POLAND

wear and corrosion resistance [10]. Rapid solidification is considered to be one of the most important methods for producing the quasicrystalline phase. This method was used to produce quasicrystalline particles in a various range of systems: Al-Mn-Ce [1], Al-Mn-Co-Ce [2], Al-Cr-Ce-Co [3], Al-Fe-Cr-Ti [4, 5] and Al-Fe-Mn-Ti [6], that exhibit high tensile strength exceeding 1000 MPa, combined with good ductility.

An aluminium-based alloy with composition $Al_{91}Mn_7Fe_2$ obtained by rapid quenching involving the melt spinning technique was reported to possess good mechanical properties with σ_f = 1250 MPa [8, 9]. Because only limited information about alloy microstructure is present in literature [11], an effort was made to perform investigations concerning the initial microstructure of the alloy in the as cast and as spun state, as well as microstructure changes after annealing. The paper presents also the study of melt-spun ribbon fabrication at different process conditions, microhardness measurements, as well as detailed study of quasicrystals transformation into stable crystalline phase during annealing.

2. Experimental

The alloy of nominal composition $Al_{91}Mn_7Fe_2$ (at. %) was prepared using high-purity elements. The alloy was cast after melting into a steel mould and then remelt and cast using the melt spinning technique. Melting and casting were performed under protective helium atmosphere. The melt was ejected onto a copper wheel rotating at three different linear velocities: v = 25, 30 and 36 m/s. The pressure of gas ejecting the molten alloy was 0.25 MPa. The microstructure of the mould cast alloy and melt spun ribbons was examined using Philips PW 1840 X-ray diffractometer (XRD) with CoK_α radiation, FEI scanning electron microscope ESEM XL30 (SEM) and FEI transmission electron microscope Tecnai G^2 (TEM) operating at 200 kV equipped with a high-angle annular dark field scanning transmission electron microscopy detector (HAADF-STEM) combined with energy dispersive X-ray (EDX) EDAX microanalysis. The Tenupol-5 double jet electropolisher was used for the thin foil preparation in an electrolyte containing nitric acid and methanol (1:3), at the temperature of -30°C and voltage of 15 V. Thermal stability of melt spun ribbons was analyzed using Du Pont 910 equipment (DSC) at a scanning rate of 40 K/min. Microhardness measurements were done by Vickers method using microhardness tester CSM Instrument with load 100 mN.

3. Results

3.1. Microstructures of initial alloys

3.1.1. Mould cast alloy

Figure 1 shows the microstructure of the alloy obtained by conventional casting into a steel mould. It consists of three phases: two phases in the form of elongated particles embedded in an aluminium solid solution. EDX results showed that the inner part of the elongated particles contains about 80% of Al, 14% of Mn and 6% of Fe and this composition corresponds to the Al_4(Mn, Fe) phase. The darker areas which surrounded Al_4(Mn, Fe) phase contains about 85% of Al, 11% of Mn and 4% of Fe and were identified as Al_6(Mn, Fe). Aluminium solid solution located between the particles contains about 1% of Mn. The mean chemical compositions of the phases are given in Table 1. Occurrence of these phases was also confirmed by XRD (Fig. 2).

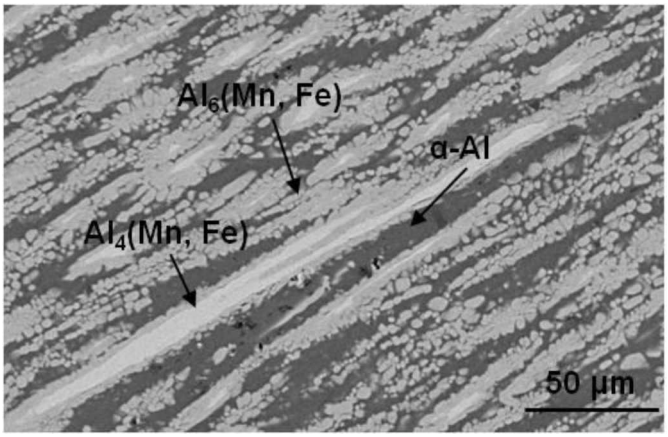

Fig. 1. Microstructure of investigated alloy in as-cast state obtained by SEM. Different phases found in microstructure are marked by arrows

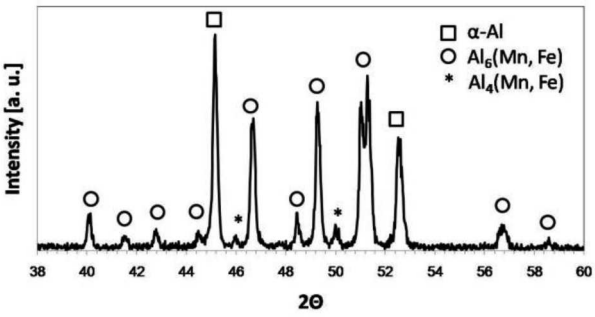

Fig. 2. XRD diffractogram presenting phase composition of cast ingot

TABLE 1
Chemical compositions of phases observed in the ingot and the melt spun ribbon. Given errors are the standard deviation from several measurements

% at.	Al	Mn	Fe
$\alpha-$Al (ingot)	99.1±0.2	0.9±0.2	–
Al_6(Mn, Fe)	85.0±0.8	11.00±1.3	4.00±0.9
Al_4(Mn, Fe)	80.1±0.7	14.3±1.0	5.6±0.9
$\alpha-$Al (melt spun ribbon)	97.3±0.8	2.01±0.7	0.6±0.3
quasicrystals (particles)	82.8±1.8	12.5±1.0	4.7±0.4
quasicrystals (eutectic)	86.2±0.9	9.4±0.8	4.4±0.5

3.1.2. Melt spun ribbons

The microstructures of the cross-sections of the melt spun ribbons obtained at different wheel speed: 25, 30 and 36 m/s are presented in Fig. 3. Although it was reported by other researches that wheel speed has major effect in promoting formation of metastable phases, like the quasicrystalline phase, it was observed that all ribbons have similar thickness in a range of 30-50 μm and similar microstructure. Two typical areas within all ribbons were shown: refine microstructure with small particles near to the wheel side of the ribbon and areas with larger dendritic particles near to the outer side which was also reported by other researchers [12]. The microstructure is not homogenous but one type of the microstructure at whole thickness has been also observed in some part of the ribbon (Fig. 3a-c). However the microstructure within the ribbon obtained with different wheel speeds is inhomogeneous in all cases it seems that with higher wheel speed more areas with refine structure was formed instead of areas filled with dendrites.

Based on the TEM investigations, including EDX microanalysis, the microstructure of the obtained melt-spun ribbons was found to consist of two phases (Fig. 4) – an aluminium solid solution with small content of manganese (up to 2 at. %) and the quasicrystalline phase with a composition similar to Al_4(Mn,Fe) (see Table 1). The size, shape and distribution of quasicrystals within the ribbons were not uniform. Quasicrystals occurred in the form of dendrites or rounded shape particles with different sizes: from hundred nanometers to several micrometers and in the form of eutectic. As was mentioned above small particles were formed favorable at the wheel-side of the ribbon, while bigger particles and dendrites including eutectic were formed rather within the outer side of the ribbon. A quasicrystalline eutectic structure was formed with slightly different composition (with lower content of Mn and the same level for Fe) compared to quasicrystals in a form of particles.

The quasicrystalline phase was recognized based on selected area diffraction patterns – both the round particles and eutectic structure revealed 2, 3 and 5 – fold symmetry, which is typical for icosahedral quasicrystals (Fig. 5). Previous investigations showed some orientation relationships between quasicrystals and an aluminium matrix due to analysis of HRTEM images and electron diffraction patterns. It was found that 5-fold axes is parallel to the <011>and <001>axes of α(Al) [13].

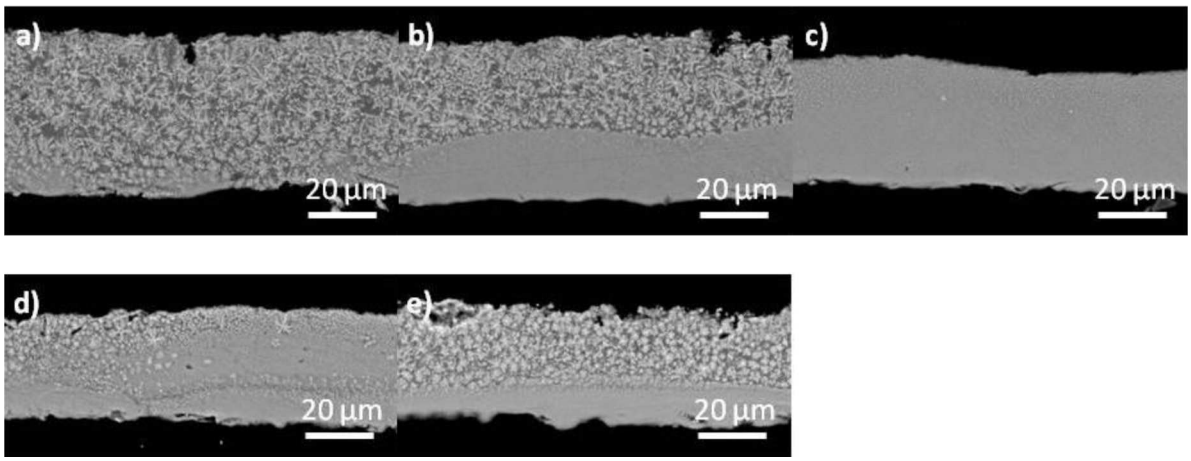

Fig. 3. SEM images of melt spun ribbons cross-section obtained at different wheel speed: 25 m/s – a), b) and c), 30m/s – d), 35 m/s – e) – showing typical inhomogeneous microstructure within the ribbon and occurrence of two typical regions with small particles and dendrites

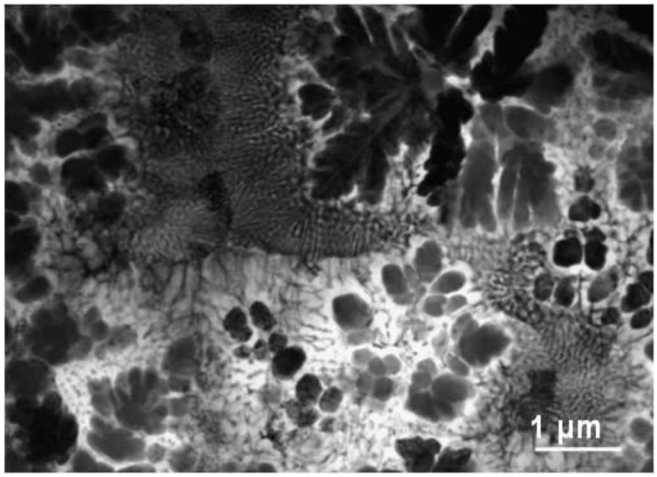

Fig. 4. Typical microstructure of melt spun ribbon obtained by TEM - BF image

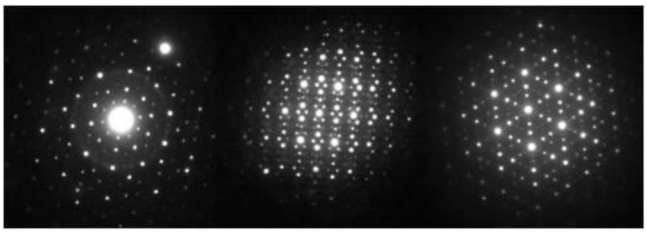

Fig. 5. Electron diffraction patterns obtained from quasicrystalline particles showing 5, 2 and 3-fold symmetry typical for icosahedral quasicrystals

3.2. Microhardness measurements

Four series of microhardness measurements were done: for ingot and melt spun ribbons obtained at different wheel speeds: 25, 30 and 36 m/s. As was expected the lowest values of microhardness were obtained for the ingot. The measured values increased for all melt spun-ribbons, although large scatter of obtained data was observed due to their inhomogeneous microstructure (Fig. 6). Areas with more refinement of the structure showed much higher microhardness values compared to areas with large dendritic particles. Based on these results, the ribbon obtained with wheel speed 30 m/s was chosen for further investigation.

3.3. Thermal stability

It is known that during annealing metastable phases like amorphous or quasicrystalline phases occurring in the melt spun ribbon transform to stable crystalline form. Temperature of transformation may be also dependent on the grain size [14]. The DSC curve (Fig. 7) shows that ribbons are stable up to 350°C which is consistent with the previous results presented in [9] .

Based on these results two temperatures were chosen for heat treatment 400 and 500°C. After annealing for 10 minutes at 400°C, only small difference in particles morphology could be noticed with the beginning of quasicrystalline phase transformation into stable crystalline phase at the quasicrystal/aluminium matrix interface (Fig. 8). After 30 min at the same temperature a significant change in the particles morphology was visible. A crystalline phase was determined as the Al_6(Mn, Fe) phase by both: electron diffraction and XRD (Fig. 9).

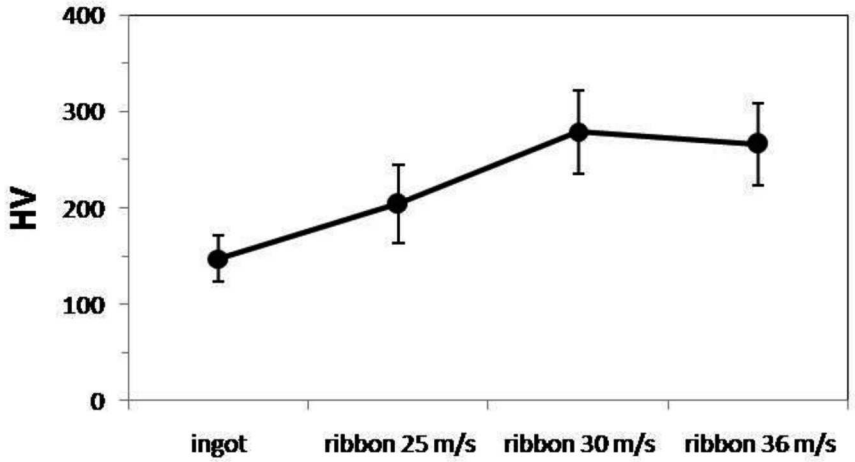

Fig. 6. Mean microhardness values for alloy in initial state marked as – ingot and in a form of melt spun ribbon produced with different wheel speed

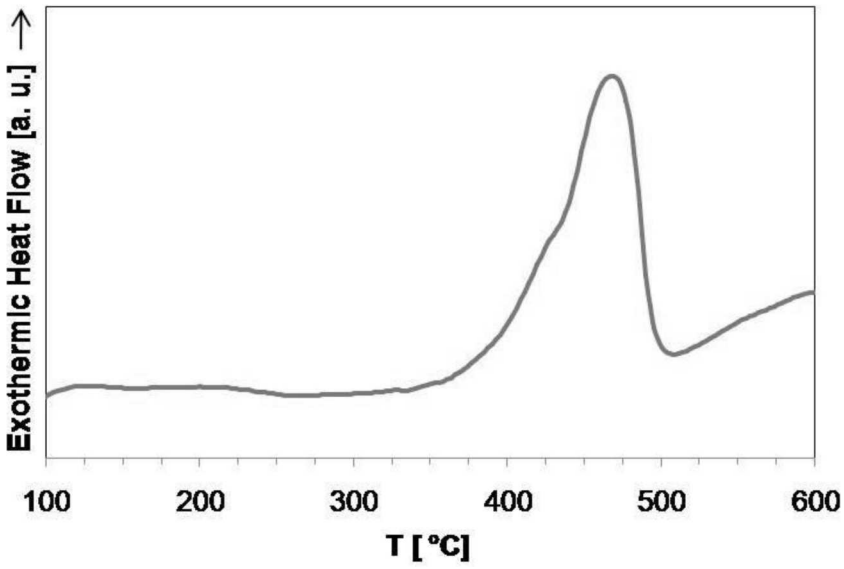

Fig. 7. DSC curve of $Al_{91}Mn_7Fe_2$ melt spun ribbon heated with the rate 40 K/min

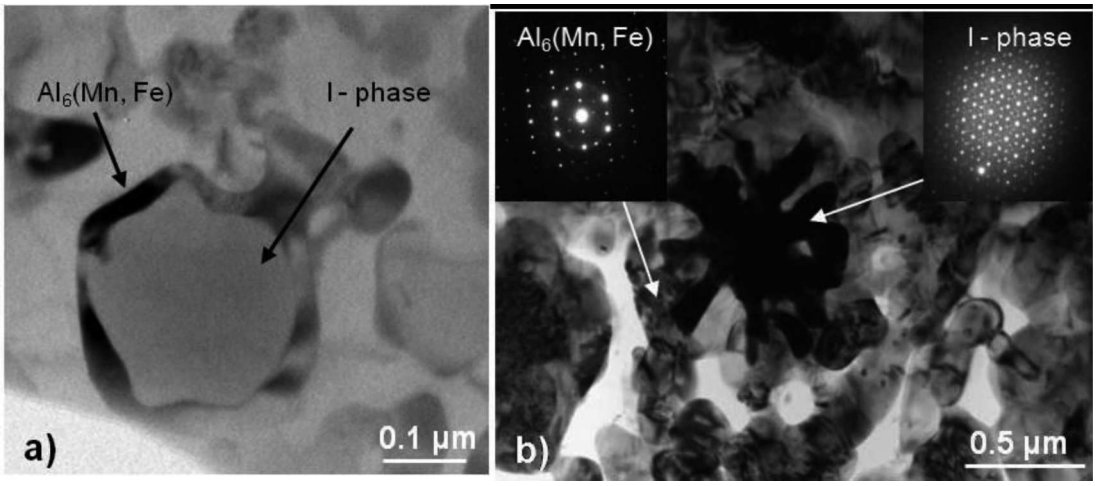

Fig. 8. Bright field images showing morphology of a) quasicrystalline particle after 10 min of annealing at 400°C, and b) after 30 min in the same temperatures. Based on SADP it can be noticed that quasicrystals transform (denoted as I-phase) into $Al_6(Mn, Fe)$ phase

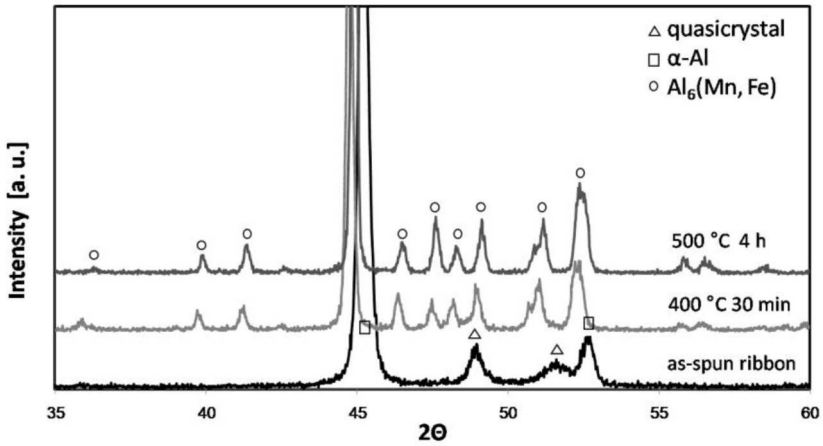

Fig. 9. XRD diffractogram showing phase composition for melt spun ribbon in as-spun state and after annealing

It was also noticed that while quasicrystalline particles were transformed only partially, quasicrystalline particles in the form of eutectic were already almost completely transformed into crystalline phase. One explanation for that is that the eutectic structure composition was closer to composition of the final Al_6(Mn, Fe) phase, comparing to the composition of quasicrystalline particles which was rather similar to the Al_4(Mn, Fe) phase. That is why transformation could be easier and thereby faster between the eutectic and Al_6(Mn, Fe) phase when assuming that only changes of atom position inside the same phase are needed. After annealing for 4 hours at 500°C, the quasicrystalline phase was completely transformed within the ribbon, so that only aluminium solid solution and Al_6(Mn, Fe) phase could be seen in their microstructure (Fig. 9).

4. Conclusion

Melt spun ribbons containing quasicrystalline particles embedded in an aluminium matrix were obtained by melt spinning with wheel rotating at different speeds. Based on electron diffraction pattern quasicrystals were identified as icosahedral (three dimensional) type. Within all kinds of ribbons, inhomogeneous structure was found with quasicrystalline particles of different sizes (from several nm to μm) and shapes (including small round particles, large dendrites, eutectic structure). Small particles were mainly placed at the wheel side of the ribbon, while large dendritic particles were mostly found at the outer side. Such microstructures occurred due to differences in undercooling within the ribbon during melt spinning process. Microstructure inhomogenity caused large scatter in measured microhardness values. Based on thermal stability investigation, it was found that quasicrystalline phase is stable up to 350°C. In higher temperatures quasicrystals starts to transform into stable crystalline Al_6(Mn, Fe) phase at the quasicrystal/aluminium matrix interface. Concerning future application of this alloy further investigation are needed to improve its thermal stability by addition of fourth element.

Received: 20 February 2012.

Acknowledgements

The work was co-financed by the European Union from resources of the European Social Fund (Project No. POKL.04.01.00-00-004/10).

REFERENCES

[1] A. Inoue, M. Watanabe, M.H. Kimura, F. Takahashi, A. Nagata, T. Masumoto, Mater Trans JIM **33**, 723 (1992).
[2] H.M. Kimura, K. Sasamori, M. Watanabe, A. Inoue, T. Masumoto, Mater. Sci. Eng. **A 181/182**, 845 (1994).
[3] A. Inoue, H.M. Kimura, K. Sasamori, T. Masumoto, Mater. Trans. JIM **35**, 85 (1994).
[4] A. Inoue, H.M. Kimura, Nanostruct. Mater. **11**, 221 (1999).
[5] M. Galano, F. Audebert, A. Garcia Escorial, I.C. Stone, B. Cantor, Acta Materialia **57**, 5120 (2009).
[6] H.M. Kimura, K. Sasamori, A. Inoue, Mater. Sci. Eng. **A 294-296**, 168 (2000).
[7] A. Inoue, H. Kimura, Sh. Yamamura, Metals and Materials International **9**, 527 (2003).
[8] A. Inoue, H. Kimura, K. Sasamori, T. Masumoto, Mater Trans JIM **37**, 1287 (1996).
[9] F. Schurack, J. Eckert, L. Schultz, Acta mater. **49**, 1351 (2001).
[10] J.M. Dubois, Mater. Science and Engineering **294-296**, 4 (2000).
[11] A. Singh, S. Ranganatha, Acta metal. Mater. **43**, 3539 (1995).
[12] F. Zupanic, T. Boncina, A. Krizman, W. Grogger, Ch. Gspan, B. Markoli, S. Spaic, J. Alloy Compd. **452**, 343 (2008).
[13] K. Stan, L. Lityńska-Dobrzyńska, J. Dutkiewicz, Ł. Rogal, A. M. Janus, TEM study of quasicrystals in Al-Mn-Fe melt-spun ribbon, Solid State Phenom. **186**, 255 (2012).
[14] R. Santamarta, A. Pasko, J. Pons, E. Cesari, P. Ochin, Archives of Metallurgy and Materials **49**, 881 (2004).